Research Inventy: International Journal of Engineering and Science
Vol.16, Issue 4 (April 2026), PP 17-28
Issn (e): 2278-4721, Issn (p):2319-6483, www.researchinventy.com

Design and Development of Aircraft Air-conditioning Cooling System Training Model for Aeronautical Engineering Students' Practice

[1]Akanimo, E. U., [2*]Assian, U. E., [3]Onuh, W. A.
[1, 3]Department of Aerospace Engineering, School of Engineering & Engineering Technology, Federal University of Technology, Ikot Abasi, Nigeria.
[2]Department of Food Engineering, College of Engineering & Engineering Technology, Michael Okpara University of Agriculture, Umudike, P. M. B. 7267, Umuahia, Nigeria.
**Corresponding Author*

Abstract: *In an effort to aid instructors to showcase different functions of an aircraft air-conditioning system and offer students in the aerospace class the opportunity for practical exercises and troubleshoot various faults in the aforementioned system, an aircraft air-conditioning cooling system (AACS) training model, based on ground-refrigeration working principle was developed. Several materials, tools and equipment used in the design, development and test performance. Major mechanical unit components included compressor, valve regulator, pressure gauge, condenser, dryer, capillary tube, fan, evaporator, etc., and were designed, modelled using SolidWorks CAD software application and fabricated. Model equations (i.e., coolingrate, heat removed from the cockpit, coefficient of performance, and convective heat transfer coefficient of the refrigerant) for measuring the AACS-training model performance were developed.Cooling monitoring and data logging unit is a microcontroller-based platform. This cooling monitoring and data logging unit comprises of sensors, AC-DC 5V converter module,Arduino Nano microcontroller, LCD display, etc., and was developed to uninterruptedly monitor, display, and record crucial environmental parameters. Preliminary test was conducted until the inner cockpit temperature was steady. The results showed that the system could reduce the cockpit mean internal temperature from 32.75 to 19.8°C.Curve got resembles a typical cooling curve, which is an indication of the system's robustness and reliability. It was suggested that AACS-training model should be operated using R134a, and holistic performance test should be carried out using global performance parameters.*

Keywords*: Design, Development, Aircraft, Air-conditioning, Cooling, Model, Students*

Date Of Submission: 07-04-2026 Date of Acceptance: 20-04-2026

I. INTRODUCTION

The prototype classic of an aircraft air conditioning system is a general utilized device in the field of aerospace engineering for training and research purposes. It preciselyreplicates the air conditioning system of an aircraft, coveringheating, cooling, and ventilation systems. By integratingappropriate aircraft components, the model enables tutors to showcase the roles of diverse system parts and offers students in the aerospace lesson the opportunity to practice and troubleshooting different faults (Norström and Hallström, 2023). This shift in trend has not only boosted student engagement and academic performance but has also offeredbetter understanding of multifaceted systems, for instance, refrigeration, energy systems, aircraft air conditioning systems, where their working principles may be difficult to comprehend(Lyngdorf*et al.,* 2024). In this case, a prototype system is required. In a typical aircraft air conditioning system, there are essential parts [environmental control system (ECS)], that aid safeguard passenger well-being. However, contemporary systems use either air-cycle machines or vapour compression refrigeration, with current research focusing on efficiency, weight reduction, and compliance to variable flight conditions.

Nevertheless, the major parts ofair-cycle machines include compressors, heat exchangers, turbines, valves, reheaters, and water separators (Merzvinskas*et al*., 2019; Zhang *et al.,* 2023; Chowdhury *et al.,* 2023). Air-cycle systems are of various types: simple**,** bootstrap**,** simple-bootstrap (3-wheel), andcondensing (4-wheel) cycle. They do not need refrigerants,are ecofriendly, andreliable under variable flight conditions.A characteristic aircraft air-cycle system works on the reverse Brayton cycle (Bell–Coleman cycle), using compressed air(Monroe Aerospace, 2022). However, vapour compression systems run like conventional refrigerating systems, which use refrigerant (e.g., R134aor other eco-friendly refrigerants), with unique components. These components work together to cool and dehumidify cabin air using bleed air from the engines(Docsity, 2018; Sen, 2024). A model of these systems could help in virtual laboratory experiments.Models are basic illustrations of real-world systems, operations, or ideas that aid in comprehending, analyzing, predicting, or designing an

object or something(Ndirika and Onwualu, 2016). They aid engineers and learners to envisage intricate systems, test concepts without real-world hazards, etc. (Ndirika and Onwualu, 2016). In engineering education, modelsbridge the gap between theory and practice; and can describes how a system behaviour under certain conditions (Norström and Hallström, 2023; Lyngdorf*et al.,* 2024).A prototyped system, that could be used as a model, must be developed based on the principles of good system designwith its peculiararchitecture(Sommerville, 2016). For instance, cooling monitoring and data logging unit whichis a microcontroller-based platform designed to uninterruptedly monitor, display, and record crucial environmental parameters within environment(Sommerville, 2016). Several hardware components such asAC-to-DC converter, Arduino Nano microcontroller, flash memory, DS18B20 digital temperature sensor, DHT21 (AM2301) digital temperature, etc.can be used (Sonal*et al.*, 2017; Arduino, 2026c).

In any typical aircraft air-conditioning cooling system model, its performance is always carried out (ASHRAE, 2019). Based on literature search, there were fewpointed thrust studies, including the proprietary works of SKYbrary Aviation Safety (2025) which offers real-time monitoring of performance of cooling system and logs data for maintenance planning operation.MadgeTech (2025) produced customizable data logging systems for aerospace applications, which enable real-time monitoring of ecological parameters such as temperature and humidity, and Phoenix Air U-15 AFL developed a research model aircraft equipped with fiber Bragg grating (FBG) sensors to monitor temperature, strain, and deformation (Phoenix Air, 2025). Ekpenyong, and Ikpe (2024) experimented on thermo-physical evaluation of hybrid-nanofluid zeotropic mixtures in a vapour compression refrigeration system, and obtained optimal global result. Also, Ekpenyong*et al.* (2023) carried out a studied on the novel design and development of a test rig for vapour compression refrigeration system (VCRS) using nanofluid-zeotropic mixtures for cooling rate mixture concentration composition between three nanofluid (CuO, TiO_2, and Al_2O_3) composition.

However, no work had developed an aircraft air-conditioning cooling system (AACS) training model for aeronautical engineering students' practice. Teaching and learning of energy, aircraft air-conditioning and refrigerating systems in numerous aerospace engineering classrooms remain mostly theoretical. This gap between theory and practice regularly deters students' ability to fully comprehend the working principles, performance characteristics, and real-time behaviour of aircraft cooling systems. The present laboratory setups, if readily accessible in anywhere, are often exclusive, or not precisely designed for instructional purposes. Again, some of these systems may lack combined monitoring and data logging capabilities, which are indispensable for analyzing system performance. Still, the absence of basic, scalable, and cost-effective prototype, fashioned for classroom use restricts empirical learning prospects. This challenge is mainly noteworthy in institutions with limited resources, where buying full-scale aircraft systems may be unrealistic. Hence, there is a need to develop a practical aircraft air-conditioning cooling system (AACS) training model, based on ground-refrigeration working principle as objective of this study. The study would give students opportunity to observe real-time system behaviour, thereby enhancing their comprehension of heat transfer and thermodynamic principles. It would improve engineering education pedagogy by offering a hands-on instructional tool that supports hands-on training and system troubleshooting.

II. MATERIALS AND METHODS

2.1 Materials, Tools and Equipment

Some major materials, tools and equipment used in the design,development and preliminary performance test of an AACS training model include L-rule, measuring tape, plump, pipe cutter, wielding flux, Oxy-acetylene cylinders with its accessories, pair of plier, saw, duct cutter, jig saw, drilling machine, vernier caliper, digital multimeter, soldering iron, soldering lead , digital anemometer and 3D-printer (as shown in Figure 1).

Figure 1: A 3-D printer

2.2 Design Concept and Considerations

The concept behind AACS- training model, is that the heat is removed from the cockpit, so that its temperature is maintained below the general temperature of its surroundings using a suitable refrigerant pumped by a compressor.The following considerations were made:

(a) The choice of material selection was based affordability and availability,
(b) The configuration of the compressor was made to cater for the continuous refilling when exhausted.
(c) The system was designed with ergonomics consideration for safer and convenient operation.
(d) The system components were appropriate and followed standards based on the computed theoretical analysis.
(e) The few system parts were constructed based on the available but durable local raw materials whereas others were bought out.

2.3 Design of an AACS-Training ModelComponents-Mechanical Unit

The trainer is furnished with necessaryparts found in an aircraft air conditioning system, including a vapour cycle compressor, compressor motor, receiver dryer, condenser, and thermal switch. For simulating the heating system, it incorporates a cooling monitoring and data captured logging unit comprises of sensors, AC-DC 5V converter module,Arduino Nano microcontroller, LCD display, that record all the necessary operation parameters. Also, the model includes vital features such as control valves;air blower; control switches, and connected ducting, for standard and efficient system operation procedures (SOPs). The SOPs enhance safety and efficiency by providing flawless instructions and guidelines for operating the trainer. By following the SOPs, users can perform tasks properly to the required standards, thereby improving the overall quality of their work.

(I) Design of the Cockpit Body

(a) Determination of External Surface Area and Volume of Cockpit

The body of the cockpit is made up of galvanized steel plate, polystyrene Styrofoam (lagging material), and aluminum plate inside as shown in Figure 2

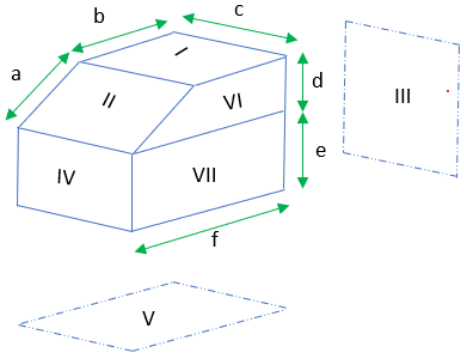

Figure 2: Dimensions of the cockpit body

If the outer dimensions are given as: a = 180 mm, b =220 mm, c = 210 mm, d = 140 mm, e = 160 mm and f = 310 mm, then the total external surface(S_{te}) is computed as (Soumya, 2024):

S_{te} = total surface areas of part I, III, IV, V, 2VI and 2VII

$S_{te} = (a \times b) + (a \times c) + (c \times [d + e]) + (c \times e) + (c \times f) + (2 \times 0.5[b + f] \times d) + (2 \times e \times f)$Eq. (1)

Then, the surface area of area glass material (S_{gm}) is represented by part II, i.e., a× c

(b) Cooling Capacity / Load in the Cockpit

The thickness of lagging material (t = 20 mm) was carefully selected to avoid heat loss or gainfromthe surrounding.However,the corresponding internal dimensions of the cockpit (Figure 2) are a* = a−2t; b* = 110 mm; c* = c− 2t; d* = d−2t; e* = e−2t; f* = 190 mm, and the volume of the cockpit (V_{CP}) is given in Equation 2 (Soumya, 2024):

V_{CP} = volume of triangular prism (V_{TP}) + volume of cuboid I (V_{CI}) + volume of cuboid II (V_{CII})Eq. (2a)

$V_{CP} = [0.5 \times (f^* - b^*) \times d^* \times c^*] + (b^* \times c^* \times d^*) + (c^* \times e^* \times f^*)$Eq.(2b)

If the volume of air in the cockpit, $V_{air} = V_{CP}$, andits density (ρ_{air}) = 1.2 kg/ m^3, then, mass of air in the cockpit (M_{air}) is given as in Equation 3 (Singh and Heldman, 2009):

$M_{air} = V_{air} \times \rho_{air}$Eq. (3)

Assuming that the maximum temperature of the cockpit that couldcause the pilot(s) discomfort is T_2 = 36ºC, time (Θ, say 3600 seconds) for the cockpit' temperature to be reduced to T_1= 6ºC (where there is comfort), air specific heat capacity (C_{pair}= 1.005 kJ/ kg ° K[Micahel*et al.,* 2020; Çengel and Bole, 2023]) and then the heat that must be removed from the cockpit ($H_{R.CP}$) was computed using Equation 3.4 (Singh and Heldman, 2009):

$H_{R.CP} = M_{air} \cdot C_{pair} \cdot (T_2 - T_1)$Eq. (4)

However, the additional heat generated from other components within the cockpit (H_{add}) must be taken away. Let the H_{add} be 50% of $H_{R.CP}$. Hence, the total heat removed from the cockpit ($H_{TR.CP}$) and the cooling rate, load or capacity (H_{Load}) were calculated using Equations 5 and6.

$H_{TR.CP}$ = 50% $H_{R.CP}$ + $H_{R.CP}$Eq. (5)

$H_{Load} = \frac{H_{TR.CP}}{\theta}$Eq. (6)

(II) Junction Box, Wire Connections, Selection of Tubing / Duct, Valve Regulator and Pressure Gauge

Junction box serves as a hub where the compressor, two fans and the electronic unittapped electrical power through wire connections. It is connected toan external power source. Copper tubing used is flexible and easy to bend. It has excellent thermal conductivity, corrosion resistance, and ability to withstand high pressure. Valve regulator is used to control the flow and pressure of refrigerant, ensuring efficient cooling, stable operation, and protection of system components. A high-pressure gauge was used as a monitoring device that measures the refrigerant pressure at different time while operating. It plays a crucial role in diagnosing performance, ensuring safety, and maintaining efficiency. These components wereall bought out.

(III) Frame Support Design

A rectangular steelframe of 40 × 40mm was used to produce the support as shown in Figure 3 with the dimensions,K_1 = 560 mm, K_2 =800 mm, K_3 = 100 mm and K_4 = 115 mm. The support is covered with mild steel plate of 3 mm thickness. At the lower part of the support is a compressor base fixed which is made of $K_4 \times K_1 \times$ 3 mm mild steel sheet. So, the total length of rectangular frame (L_{RF}) and the total surface area of the mild steel plate (A_{SP}) were calculated using Equations 7 and 8 respectively (Soumya, 2024):

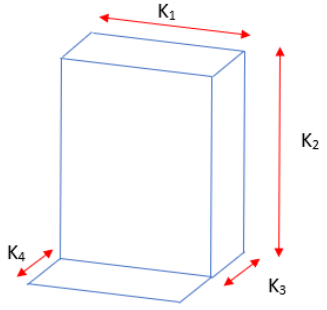

Figure 3: Frame support.

$L_{RF} = 4 \times K_1 \times K_2$Eq. (7)

$A_{SP} = 2\,[(K_1.K_3) + (K_3.K_2) + (K_1.K_2)]$ Eq.(8)

2.5 Production of AACS-Training Model

The orthographic projection, exploded, 3D models and pictorial views of AACM/ DLSwas generated using SolidWorks CAD software application.

2.6 Fabrication Phase II-Coupling of Cooling Monitoring / Data Logging Unit

A customized, designed 3D-printed enclosure was fabricated from polyethylene terephthalate glycol (PETG) filament (Megan, 2026). It is architecturally divided into two primary compartments: display compartment (upper section) and circuit compartment (lower / hollow section). The customized 3D-printed enclosurewas precisely-cut and recessed to house the 20 × 4 LCD module. It was bezel integrated with transparent window for clear viewing of displayed parameters, mounted with four posts with self-tapping screw holes to secure it, and beveled edges at 15° for improved aesthetics and ergonomic viewing angle. Spacious hollow cavity was designed to accommodate: Arduino Nano microcontroller (secured via standoffs), SD card module (positioned near access slot), AC-DC 5V converter which was thermally isolated, Veroboard with soldered connections (elevated on standoffs), wiring harness and connectors (routed through channels), ventilation slots for passive cooling of power supply components, SD card access slot for easy removal without opening the enclosure, (the slot includes a spring-loaded cover to prevent dust ingress when not in use), and two PG7 cable glands for sensor and power cable entry/exit for: AC power input cable, DS18B20 sensor cable, and DHT21 sensor cable.

2.7 Parameters and Models forMeasurement of AACS-Training Model Performance

The following global parameters were used to measure the AACS-training model performance:

(a) Pressure of the refrigerant from the compressor to the condenser;
(b) Internal and external temperatures of the cockpit;
(c) Humidity of the cockpit;
(d) Cooling rate and heat removed from the cockpit;
(e) Coefficient of performance; and
(f) Convective heat transfer coefficient of the refrigerant.

(I) Pressure of the Refrigerant from the Compressor to the Condenser

This parameter was read or visually monitored using a high-pressure gaugethat is installed between the compressor to the condenser while on operation.

(II) Internal, External Temperatures and Humidity of the Cockpit

The internal and humidity of the cockpit were sensed and documented using a combined temperature-humidity sensor whereas the external or environmental temperature was read by a temperature sensor.

(III) Cooling Rate and Heat Removed from the Cockpit

Coolingrate (Q_r) is the rate at which an air-conditioning system removes heat from a space. From Equation 4, we haveQ_r as the model represented in Equation 9 (Singh and Heldman, 2009):

$$Q_r = \rho_{air}.v_{air}.A_{air}.C_{pair}.\Delta T \quad \text{Eq. (9)}$$

$$A_{air} = \frac{\pi.d_{fan}^2}{4} \quad \text{Eq. (10)}$$

where, ρ_{air} = density of air (1.2 kg /m^3), v_{air}= air velocity produced from the fan (5.6 m/s as measured using anemometer), A_{air} = cross circular sectional of fan with blade diameter (Soumya, 2024),d_{fan} = fan blade diameter= 12 cm = 0.12 m, C_{pair}= air specific heat capacity (1.005 kJ/ kg °K), ΔT is the difference in minimum inside temperature of the cockpit (T_i), and external or outside temperature of the cockpit (T_o) which was the variable.

Therefore, heat removed from the cockpit (H_r) at certain period, *t* (in sec) was computed in the model Equation 11 (Singh and Heldman, 2009).

$$H_r = Q_r.t \quad \text{Eq. (11)}$$

(IV) Coefficient of Performance (COP)

This parameter is used to describe heating or cooling efficiency of a system. It is given as (Izham*et al.,* 2010; Johra, 2022):

$$COP = \frac{Q_r\ (kW)}{\text{Compressor electrical power}\ (kW)} \text{[in decimal]} \quad \text{Eq. (12)}$$

$$\text{Compressor electrical power} = \text{voltage} \times \text{current} \quad \text{Eq. (13)}$$

But voltage and current that passed across it were measured as 230 volt and 0.6 Amperes respectively using multimeter. Hence, the model for measuring COP was derived from Equation 12.

(V) Convective Heat Transfer Coefficient of the Refrigerant

Convective heat transfer coefficient of the refrigerant (h) measures how heat is effectively transferred between the refrigerant and the surrounding. The model is given as (The Engineering Toolbox, 2026):

$$h = \frac{Q_r\ (W)}{A_T\ (\text{Abs}\ [T_{wall} - T_{ref}])} (\text{in}\ w/m^2.K) \quad \text{Eq. (14)}$$

where, A_T = total surface area of the inner evaporator tube with length, L_e= 1.95 m and diameter,d_e= 0.004 m (measured),T_{wall} = wall temperature of the tube (2°C), andT_{ref} = the temperature of the refrigerant in the evaporator (5.5°C) (ASHRAE, 2022).

But $A_T = L_e.\pi.d_e$ Eq. (15)
Model Equations 9, 11, 12 and 14were used intheaircraft air-conditioning cooling monitoring and data logging system.

2.8 Overview of Cooling Monitoring and Data Logging Unit

The cooling monitoring and data logging unitis a microcontroller-based platform designed to uninterruptedly monitor, display, and record crucial environmental parameters withinenvironment.The system architecture is organized into four major functional units:power supply,processing andoutput and storage.

2.8.1 Hardware Components

Some of the hardware components used include:(a)- Arduino Nano microcontroller, (b)- Output and display unit- 20×4 LCD character display with I2C interface, (c)- AC-DC 5V converter module, (d)-Flash memory, (e)- Micro SD card module with level shifter, (f)- 74HC125D quad level shifter (integrated on module),(g)-DS18B20 digital temperature sensor (outside / evaporator), (h)-DHT21 (AM2301) digital temperature and humidity sensor (inside/ambient), (i)-Micro SD card, and (j)-Veroboard as shown in Figure 4.

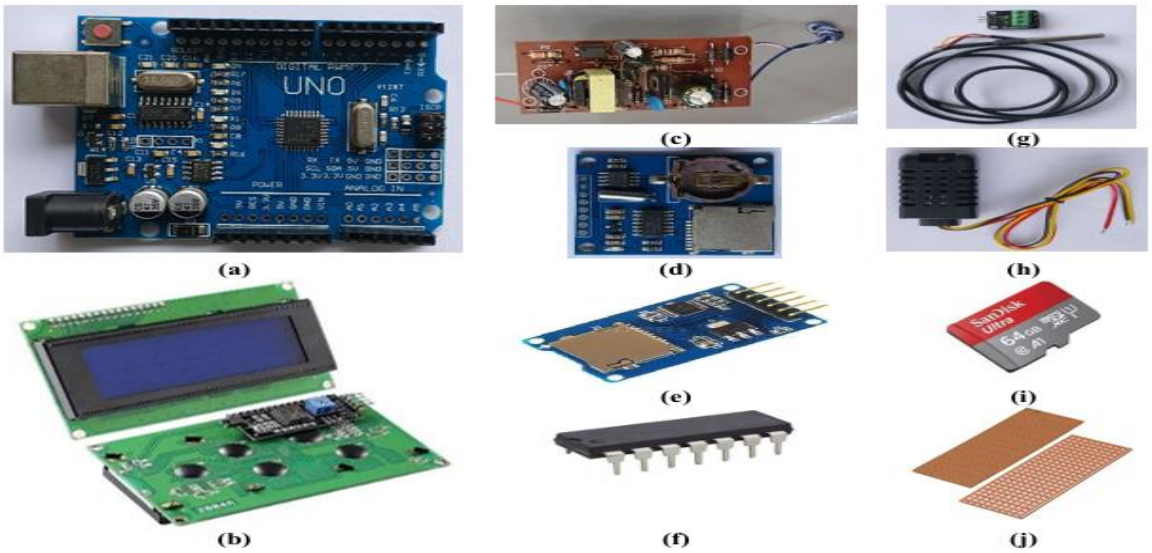

Figure 4: Some major hardware components used in control unit.

2.9 System Block Diagram and Operation

The system block diagram (Figure 5) illustrates the functional architecture.

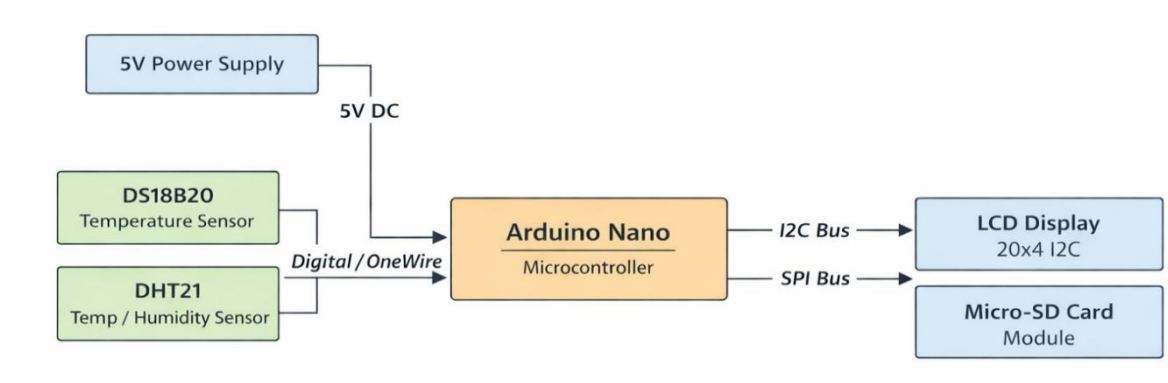

Figure 5: Complete system block diagram

From Figure 5, the AC-to-DC converter transforms the mains AC 5 V into a stable 5V DC output, which is suitable for low-power electronic components (Nantian Electronics, 2024). The sensor unit is responsible for collecting environmental data required for monitoring the system. Two sensors are used in this design are DS18B20 temperature sensor and DHT21 temperature and humidity sensor. Together, these sensors form the data acquisition stage of the system.The processing unit is the central component of the system and is

implemented using the Arduino Nano microcontroller(central controller) (Arduino, 2026a).The Arduino Nano microcontrollerperforms several critical tasks, including: acquiring temperature data from the DS18B20 sensor; acquiring temperature and humidity data from the DHT21 sensor; processing the sensor data, performing system calculations and data formatting; and managing communication with output devices, and controlling data storage operations.The microcontroller acts as the central controller, coordinating the flow of information between sensors, display modules, and storage devices.The output and data storage unit allow users to view system data in real time and store them for later analysis. These composed of LCD display and micro-SD card storage units.A 20×4 LCD display with an I2C interface is used to present system parameters to the user (Arduino, 2026b). The display communicates with the Arduino via the I2C bus, which simplifies the wiring by using only two communication lines. The LCD provides real-time visualization of the measured parameters, enabling the user to monitor system conditions during operation.The micro-SD card module is used for data logging purposes. It communicates with the Arduino Nano through the serial peripheral interface (SPI) bus (Arduino, 2026c). The system periodically records sensor readings and calculated parameters and stores them on the SD card in CSV format. This format allows the recorded data to be easily imported into analytical tools such as Microsoft Excel, Python, or other data analytical software packages. However, the system operational flowchart is shown in Figure6.

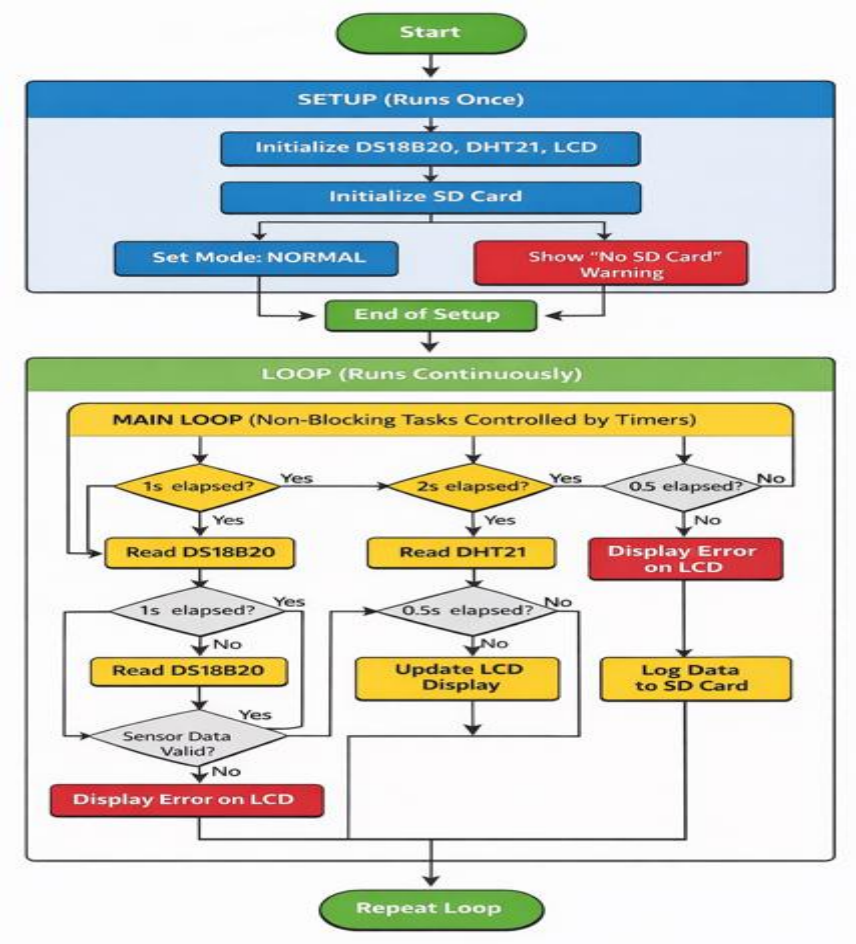

Figure 6: System operational flowchart

The operational sequence begins with system initialization, including hardware configuration and SD card detection. Based on SD card status, the system enters either ***Normal Mode*** (data acquisition, display, and logging) or ***Warning Mode*** (visual alert). The main loop continuously executes non-blocking tasks according to the timing specifications, time-sliced task scheduler and non-blocking scheduling pattern using the millis () function as shown in Table 1 and Figure 7 (Brewer, 2024; Rosing, 2024).

Table 1: System task scheduling

Task ID	Description	Trigger Condition	Interval	Action Performed
T1	Read DS18B20 Temperature Sensor	(currentMillis - lastTempRead>= intervalTemp)	1 second	Acquire evaporator/outside temperature measurement (Tout)
T2	Read DHT21 Temperature & Humidity Sensor	(currentMillis - lastDHTRead>= intervalDHT)	2 seconds	Acquire ambient/inside temperature (Tin) and relative humidity (RH)
T3	Perform System Calculations	(currentMillis - lastCalc>= intervalCalc)	1 second	Calculate cooling rate (Q), heat removed (Hr), COP, and thermal coefficient (h)
T4	Update LCD Display	(currentMillis - lastDisplay>= intervalDisplay)	0.5 seconds	Refresh real-time system values on 20×4 LCD with proper formatting
T5	Log Data to SD Card	(currentMillis - lastSDWrite>= intervalSD)	10 seconds	Store sensor and calculated values to CSV file with 2-decimal precision
T6	Sensor Validation Check	After each sensor read	Immediate	Verify sensor data validity; set error flags if invalid

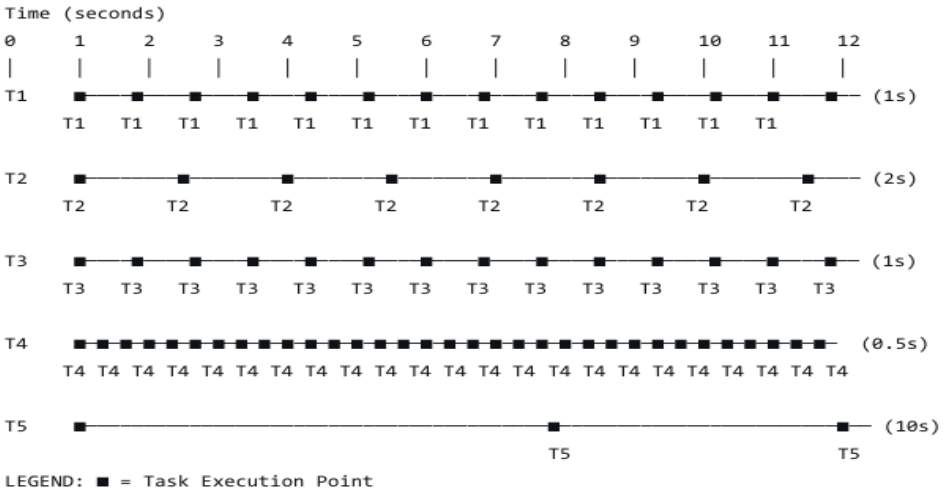

Figure7: Task execution timing diagram

Input /output blocking was mitigated via primary design, and the concurrency strategy was employed to allow eachtask to be evaluated independently. System robustness and failsafe architecture such as exception handling strategy, graceful degradation, watchdog timer configuration, and data integrity and validationwere employed to prevent reporting inaccurate data during hardware faults.

2.10 Working Principleof AACS Training Model

As soon as power is switched on, the system delays a bit and the compressor begins discharging the refrigerant from a low-pressure saturated vapour to a high-pressure superheated vapour under constant entropy conditions through the discharged duct. The regulator valve, installed along the duct, allows certain amount of the refrigerant to pass through a high-pressure gauge. The condenser sub-cools the high-pressure superheated gas to a saturated vapour state, which is then condensed into a saturated liquid state under constant pressure. At this stage, the refrigerant temperature reduces and passes to the dryer. At thisstage, the moist vapour in the duct tube is expanded to a low pressure and temperature liquid-vapour mixture at constant enthalpy. This further reduces the refrigerant temperature as it gets into the capillary tube. At the evaporator, the low-pressure two-phase mixture boils to saturated vapour under constant pressure, and the refrigerant absorbs heat from the cockpit and sends it back the compressor for recycling. Simultaneously, as the system is powered, the external and internal temperatures, and humidity of the cockpit are monitored by the sensors, displayed on the LCD screen and stored in micro SD card. Also, values of period of operation, cooling rate, heat removed from the cockpit, coefficient of performance (COP) and convective heat transfer coefficient of the refrigerant are displayed and stored.

2.11 Preliminary Simulation Performance of the Training Model

After assembling, the system was powered on for 15 minutes. This allowed for careful examination to be sure that the system was perfectly coupled. Faults noted were corrected and system was allowed for 20

minutes to achieve room temperature conditions. Thereafter, the valve regulator was opened to a full scale, the system turned on, and allowed to run. The system inner cockpit temperature, as well as other parameters, was monitored on the liquid crystal display (LCD), at certain time interval, t in seconds, until there was no tangible change in the inner cockpit temperature. This period was noted and used a guide in further experimentations. Then, the variation of inside temperature of the cockpit of the prototyped aircraft air-conditioning coolingsystem embedded with monitoring and data logging systemagainst cooling time was made, using Microsoft Excel ™and physically compared to a known cooling curve in order to ascertain the system level of effectiveness.

III. RESULTS AND DISCUSSION

3.1 Results

The results of the study are presented in this chapter and subsequently discussed.

(I) Specifications of the Components

(a) Cockpit Body

S_{te}= 381300 mm^2

S_{gm} = a*c = 37800 mm^2

(b) Parameters and Models Applied in Cooling Monitoring and Data Logging Unit

$Q_r = 0.076391 \times (T_o - T_i)$ [in J/sec or W] Eq.(16)

$Q_r = 0.000076391 \times (T_o - T_i)$ [in kJ/sec or kW] Eq.(17)

$H_r = 0.076391 \times (T_o - T_i) \times t$ [in J]Eq.(18)

$H_r = 0.000076391 \times (T_o - T_i) \times t$ [in kJ]Eq.(19)

Compressor electrical power = 0.138 kW

$COP = \frac{Q_r\ (kW)}{0.138\ (kW)}$ [in decimal] Eq.(20)

$A_T = 0.0245076$ m^2

Absolute = 3.5^{o}C or 3.5 K

$h = \frac{Q_r\ (W)}{0.085776\ (m^2.K)}$Eq.(21)

ModelEquations16 to 21 were used inthedeveloping AACS training model.

(II) Models and Pictorial Views of the AACS Training Model

The 3-D model and pictorial view are presented in Figures 8.

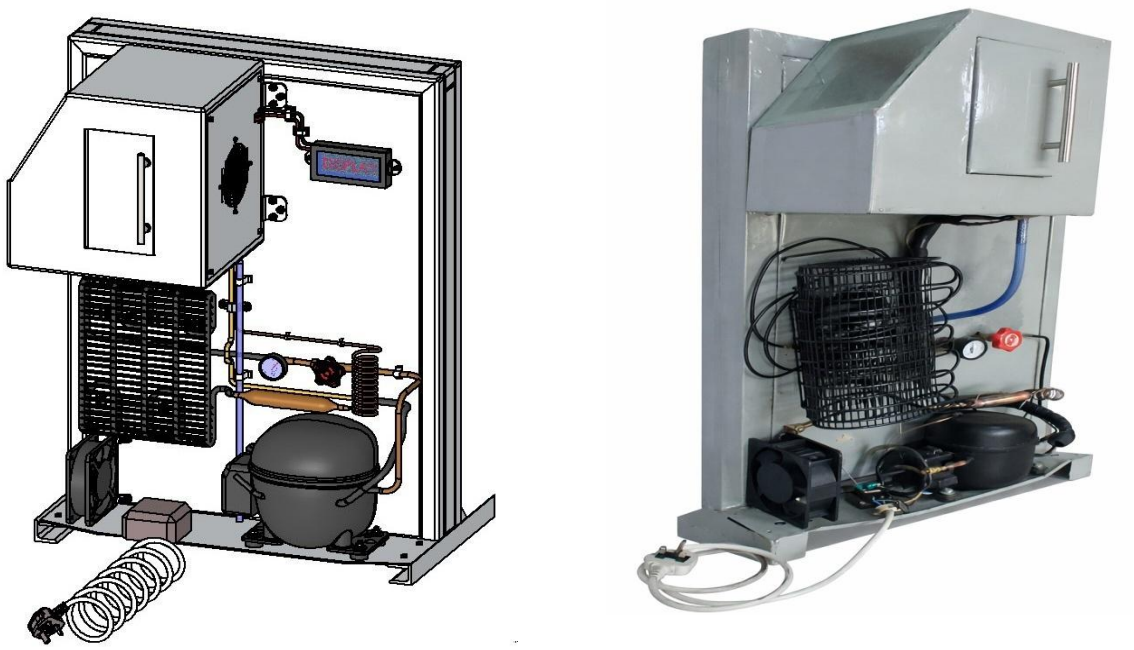

(i) **(ii)**

Figure 8: (a)3-D model, and (b) Pictorial view of the AACS training model.

(III) Performance Evaluation

The pictures got from the LCD are shown in Figures 9.

(i) The display when the system just starting

(ii) The display after 4 seconds of start

Figure 9: Display when the system just starting and after 4 seconds

However, the variation of inside temperature of the cockpit of a prototype AACS training modelagainst cooling time, also known as cooling curve is presented in Figure 10.

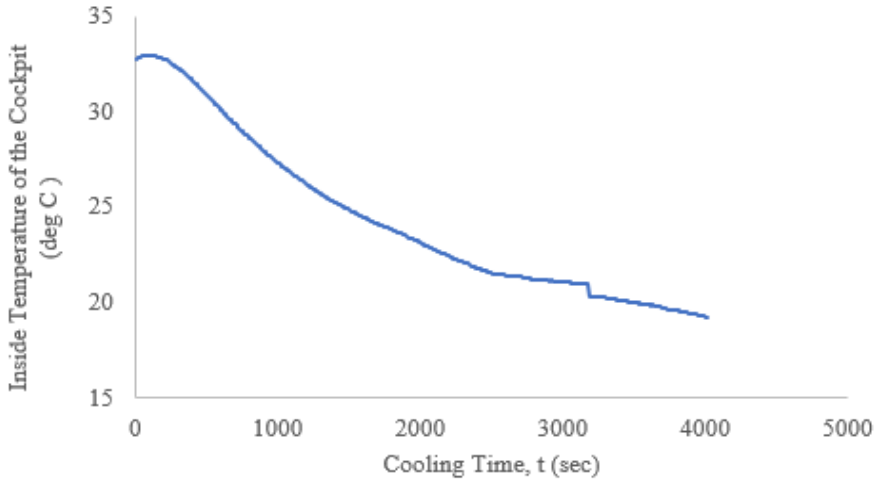

Figure 10: Inside temperature of the cockpit against coolingtime-cooling curve

The display in Figure 9 was got from certain experimentation, after the trial run. It is just to show how the LCD displays the reading and computed parameters. From Figure 10, the maximum inside temperature of the cockpit before the system was powered was 28.7°C. At about 1003 seconds of cooling, the temperature had dropped to 24.9°C. Exactly 19.8°C was recorded at the cooling period of 4009 seconds. There was a slight increase in temperature to 20.1°C. This might have been as a result of opening the cockpit to physical have first -hand feeling by the researcher.

3.2 Discussion of the Findings

(I) Specifications of the Components

All the specifications derived from the design calculations and analyses were used to select or source for the system components. Other components were chosen based on their availability, unique specifications, and enough factor of safety to avoid failure during stress or operation. Besides, these components were also used to generate orthographic and exploded views, 3-D model and pictorial view of the training modelfor easy fabrication.

(II) Preliminary Performance Evaluation Test

As the cooling time was increased in Figure 10 there was initial rapid cooling process where, the temperature difference between the cockpit and the surrounding was large; hence, heat was quickly removed. So, temperature fell rapidly. As the cockpit got cooler, the temperature difference decreased, therefore, heat removal was reduced. So, the cooling curve becomes less steep, and eventually, temperature fell to 19.8°C and almost constant after 4009 seconds. The observed curve resembles a typical cooling curve which implies that the system could efficiently cool a cockpit if the design is scale up. The result of the present study is similar to Kumar *et al.*(2022). They investigated refrigerator channel performance in liquid rocket engines, and found that temperature decreased as the cooling time increased because of heat transfer. Also, Dinh*et al.* (2024) revealed that cooling rate depends on space size and lagging material; lower target temperatures require longer cooling times.

IV. CONCLUSION

In this study, an aircraft air-conditioning cooling system (AACS) training modelbased on ground-refrigeration working principle was developed, using specified mechanical refrigeration and some electronic components, for use in aerospace classroom teaching, learning and laboratory experimentations.Preliminary test was conducted until the inner cockpit temperature was steady. The results showed that the AACS training model could reduce the cockpit mean internal temperature from 32.75 to 19.8^{o}C. The curve got from the preliminary test resembles a typical cooling curve, which is an indication that the system could provide a robust, reliable, and professional platform for continuous environmental monitoring. It was recommended that the system should be operated with the refrigerant such as R134a, and further holistic performance test should be carried out.

Conflict of Interest

There is no conflict to disclose.

ACKNOWLEDGEMENT

The authors are grateful to FederalUniversity of Technology, Ikot Abasi,Institutional-Based Research (IBR),TETFUND Unit, for thefundprovided and the facilities made available for the research work.

REFERENCES

[1]. *Arduino, 2026a.* Nano – Arduino Docs. *Arduino.* https://docs.arduino.cc/hardware/nano(Retrieved on 28th March 2026)

[2]. *Arduino, 2026b.* Liquid Crystal Library – Arduino Documentation. Arduino. https://docs.arduino.cc/libraries/liquidcrystal (Retrieved on 28th March 2026)

[3]. *Arduino, 2026c.* SD Library – Arduino Documentation. Arduino. https://docs.arduino.cc/libraries/sd(Retrieved on 28th March 2026)

[4]. ASHRAE, 2019. ASHRAE Handbook—HVAC Applications (SI) https://www.ashrae.org/file%20library/technical%20resources/covid19/si_a19_ch13.pdf? utm_source=copilot.com

[5]. ASHRAE, 2022. *ASHRAE Handbook – Refrigeration*. American Society of Heating, Refrigerating and Air-Conditioning Engineers (ASHRAE), Atlanta, GA.

[6]. Brewer, F., 2024. Lecture 7: Real-time Task Scheduling. University of California, Santa Barbara. https://www.ece.ucsb.edu/ (Retrieved on 28th March 2026)

[7]. Çengel, Y. A. and Bole, M. A., 2023. Thermodynamics: An Engineering Approach (10th Ed.). McGraw-Hill Education, New York, USA.

[8]. Chowdhury, S. H., Ali, F. and Jennions, I. K., 2023. A review of aircraft environmental control system simulation and diagnostics. *Proceedings of the Institution of Mechanical Engineers, Part G: Journal of Aerospace Engineering, 237*(11): 2453–2467.

[9]. Dinh, T. H., Le, T. H. N. and Nguyen, T. H. (2024). Research, design, manufacture cooling system for test chamber. In Proceedings of the 3rd Annual International Conference on Material, Machines and Methods for Sustainable Development (MMMS2022). *Springer:* 499–506.

[10]. Docsity, 2018. *Aircraft Refrigeration*. Docsity. Retrieved March 30, 2026, from https://www.docsity.com

[11]. Ekpenyong, A. U., and Ikpe, E. A., 2024. Thermo-physical Evaluation of Hybrid-Nanofluid Zeotropic Mixtures in a Vapour Compression Refrigeration System. Gumushane University Journal of Science and Technology; 14(4): 1021-1038

[12]. Ekpenyong, A. U., Fidelis, I. A., and Aniekan, E. I., 2023. A Novel Design and Development of a Test Rig for Vapour Compression Refrigeration System (VCRS) using Nanofluid-Zeotropic Mixtures. ICONIITECHII Journal. 7th International Conference on Innovative Surveys in Positive Sciences. July 4-5. Ankara, Turkey, 7(13): 34-45

[13]. Izham, M. N. and Mahlia, T. M. I. (2010). Effect of ambient temperature and relative humidity on COP of a split room air conditioner. Journal of Energy and Environment, 2(1):33–38**.**

[14]. Johra, H., 2022. Overview of the Coefficient of Performance (COP) for conventional vapour-compression heat pumps in buildings. Department of the Built Environment, Aalborg University: Aalborg, Denmark.

[15]. Kumar, S. S. and Rajan, R. R., 2022. Heat transfer analysis of coolant channel in liquid rocket engine. International Journal of Research Publication and Reviews, 3(12): 680–684.

[16]. Lienhard, J. H. IV and Lienhard, J. H., V., 2024. A Heat Transfer Textbook (6th ed.). Phlogiston Press, Cambridge, MA.

[17]. Lyngdorf, N. E. R., Jiang, D. and Du, X., 2024. Frameworks and models for digital transformation in engineering education: A literature review using a systematic approach. Education Sciences,14(5): 519. https://doi.org/10.3390/educsci14050519

[18]. MadgeTech, 2025. Data logging solutions aerospace industry. MadgeTech. Retrieved April 1, 2026, from https://www.madgetech.com

[19]. Megan, C., 2026. PETG 3D Printing Filament: Materials, Properties, and Uses. https://www.xometry.com/resources/3d-printing/petg-3d-printing-filament/

(Retrieved on 28th March 2026)

[20]. Merzvinskas, M., Bringhenti, C., Tomita, J. T. and de Andrade, C. R., 2019. Air conditioning systems for aeronautical applications: A review. *The Aeronautical Journal,* 124(1274): 1274–1298.

[21]. Michael, J. M., Howard, N. S., Daisie, D. B. and Margaret, B. B., 2020. Fundamentals of Engineering Thermodynamics (9th Edition).Wiley, Hoboken, New Jersey, USA.

[22]. Monroe Aerospace, 2022. Air Cycle Machines: How Airplanes Regulate Cabin Air. https://monroeaerospace.com (Retrieved on 30, March 2026)
[23]. Nantian Electronics, 2024. A Complete Guide to AC/DC Converter.Nantian Electronics. https://www.nantian-electronics.com/ac-dc-converter-guide (Retrieved on 28th March 2026)
[24]. Ndirika, V. I. O. and Onwualu, A. P., 2016. Design Principles of Post-harvest Machines. 1st Edition. Naphtali Prints, Lagos, Nigeria, 323p.
[25]. Norström, P. and Hallström, J., 2023. Models and modelling in secondary technology and engineering education. International Journal of Technology and Design Education,33(5): 1797–1817.
[26]. Phoenix Air, 2025. Aircraft Condition Monitoring System (Advanced Flying Laboratory*)*. (Retrieved April 1, 2026.)
[27]. Rosing, T. S., 2024. Timing and Scheduling. Department of Computer Science and Engineering, University of California, San Diego. https://cseweb.ucsd.edu/~trosing/ (Retrieved on 28th March 2026)
[28]. Shen, H. and Xiugan Yuan, X., 2011. The Application of the Human Model in the Thermal Comfort Assessment of Fighter Plane's Cockpit. In: V.G. Duffy (Ed.): Digital Human Modeling, Springer-Verlag Berlin Heidelberg, 6777: 357–366.
[29]. Singh, R. P. and Heldman, D. R., 2009. Introduction to Food Engineering. 4th Edition. Academic Press Publication, China, 864p.
[30]. SKYbrary Aviation Safety, 2025. Aircraft Condition Monitoring System (ACMS).SKYbrary. Retrieved April 1, 2026, from https://www.skybrary.aero
[31]. Sommerville, I., 2016. Software Engineering (10th ed.). Pearson. Boston
[32]. Sonal, C., Priya, K., Shruti, S., Prajakta, P., Snehal, S. and Shweta, M., 2017. Real time smart city garbage collection and monitoring system usingGSM and GPS.International Research Journal of Engineering and Technology (IRJET), 4(3): 1226 -1229.
[33]. Soumya, D., 2024. Mensuration Formulas PDF for All 2D, 3D Shapes in Maths, Get Chart https://www.adda247.com/school/author/soumyadeep/ (Retrieved on 27th March 2026)
[34]. The Engineering Toolbox, 2026. Metabolic Heat Gain from Persons https://www.engineeringtoolbox.com/metabolic-heat-persons-d_706.html (Retrieved on 12 March 2026)
[35]. Zhang, H., Wu, Q., Feng, S., Dong, S. and Gao, Z., 2023. Vapour compression refrigeration system for aircrafts: Current status, large-temperature-range challenges and emerging auto-cascade refrigeration technologies. Aerospace,12(8): 681. MDPI. https://doi.org/10.3390/aerospace12080681